Cell

Elongator Controls the Migration and Differentiation of Cortical Neurons through Acetylation of α-Tubulin

Catherine Creppe,[1,8] Lina Malinouskaya,[2,8] Marie-Laure Volvert,[2] Magali Gillard,[1] Pierre Close,[1,7] Olivier Malaise,[2] Sophie Laguesse,[2] Isabelle Cornez,[1] Souad Rahmouni,[3] Sandra Ormenese,[4] Shibeshih Belachew,[2,5] Brigitte Malgrange,[2] Jean-Paul Chapelle,[1] Ulrich Siebenlist,[6] Gustave Moonen,[2,5] Alain Chariot,[1,9,*] and Laurent Nguyen[2,9,*]
[1]GIGA-Signal Transduction
[2]GIGA-Neurosciences
[3]GIGA-Infection, Immunity, and Inflammation
[4]GIGA-Imaging and Flow Cytometry
[5]Department of Neurology
University of Liege, C.H.U. Sart Tilman, 4000 Liège, Belgium
[6]Laboratory of Immunoregulation, National Institute of Allergy and Infectious Diseases, National Institutes of Health, Bethesda, MD 20892-1876, USA
[7]Present address: Clare Hall Laboratories, Cancer Research UK London Research Institute, Blanche Lane, South Mimms EN6 3LD, UK
[8]These authors contributed equally to this work
[9]These authors contributed equally to this work
*Correspondence: alain.chariot@ulg.ac.be (A.C.), lnguyen@ulg.ac.be (L.N.)
DOI 10.1016/j.cell.2008.11.043

SUMMARY

The generation of cortical projection neurons relies on the coordination of radial migration with branching. Here, we report that the multisubunit histone acetyltransferase Elongator complex, which contributes to transcript elongation, also regulates the maturation of projection neurons. Indeed, silencing of its scaffold (Elp1) or catalytic subunit (Elp3) cell-autonomously delays the migration and impairs the branching of projection neurons. Strikingly, neurons defective in Elongator show reduced levels of acetylated α-tubulin. Reduction of α-tubulin acetylation via expression of a nonacetylatable α-tubulin mutant leads to comparable defects in cortical neurons and suggests that α-tubulin is a target of Elp3. This is further supported by the demonstration that Elp3 promotes acetylation and counteracts HDAC6-mediated deacetylation of this substrate in vitro. Our results uncover α-tubulin as a target of the Elongator complex and suggest that a tight regulation of its acetylation underlies the maturation of cortical projection neurons.

INTRODUCTION

The generation of cerebral cortical neurons is a complex process that relies on the decision of progenitors to leave the cell cycle, migrate to appropriate laminar locations, and differentiate into neurons that are stably positioned and are actively extending axonal and dendrite branches. Importantly, these concurrent steps imply dynamic cell shape remodeling which largely depends on the regulation of cytoskeleton components (da Silva and Dotti, 2002; LoTurco and Bai, 2006; Shu et al., 2006). Thus, identification of new cytoskeleton regulators is essential to shed more light on the molecular mechanisms responsible for the generation of fully differentiated cortical neurons. Here, we investigate the contribution of Elongator in cerebral corticogenesis.

This highly conserved complex of six subunits (Elp1–Elp6) was identified associated with hyperphosphorylated form of yeast RNA polymerase II (Hawkes et al., 2002; Kim et al., 2002) and is assembled by the scaffold protein Elp1 (Close et al., 2006; Petrakis et al., 2004). Elp3, the catalytic subunit, harbors motifs found in the GNAT family of histone acetyltransferases (HATs) (Wittschieben et al., 1999) and acetylates histone H3 (Hawkes et al., 2002; Kim et al., 2002; Winkler et al., 2002). Elongator associates with several nascent RNAs in yeast (Kristjuhan and Svejstrup, 2004) and is preferentially recruited to the transcribed regions of human genes (Close et al., 2006; Kouskouti and Talianidis, 2005), which supports a role for this complex in transcript elongation. Other reports also provided evidences for a role of Elongator in exocytosis and tRNA modification in the cytoplasm (Esberg et al., 2006; Huang et al., 2005; Rahl et al., 2005). Although these reports brought insights into the roles of Elongator, it is unclear whether this complex harbors multiple functions in distinct cell compartments or whether a single function indirectly regulates the others (Svejstrup, 2007).

Elongator deficiency in humans causes familial dysautonomia (FD), an autosomal recessive disease characterized by defects in the development and maintenance of neurons of the autonomic and sensory systems (Axelrod, 2004; Slaugenhaupt and Gusella, 2002). FD results from a mutation in a splice acceptor site of the ELP1-encoding gene, *IKBKAP*, which causes exon skipping and expression of a truncated and unstable mRNA transcript. As

a result, levels of ELP1 are decreased in a tissue-specific manner (Anderson et al., 2001; Slaugenhaupt et al., 2001). Although the molecular and cellular mechanisms underlying this disorder remain largely undefined, reduced cell motility may account for this disease because a variety of human cells depleted for ELP1 harbor defects in cell migration (Close et al., 2006).

In the present study, we show that Elongator is expressed in the cytoplasm of cortical projection neurons, where it regulates radial migration and branching. Acetylated α-tubulin levels are reduced in cortical neurons as well as in various other Elongator-deficient cell types, and both Elp1 and Elp3 interact with microtubules. In addition, a purified Elp3-enriched fraction promotes the α-tubulin acetylation in vitro, and Elp3, but not Elp3ΔHAT, counteracts HDAC6-mediated α-tubulin deacetylation in vivo. Importantly, overexpression of the nonacetylable dominant-negative α-tubulin K40A mutant impairs the migration and branching of projection neurons without worsening the corresponding defects that result from Elongator loss of function, which suggests that a tight regulation of α-tubulin acetylation by Elp3 is critical for Elongator to promote the migration and differentiation of projection neurons during corticogenesis.

RESULTS

Elongator Subunits Are Expressed in the Developing Cerebral Cortex

On the basis of a previous study reporting the expression of Elp1 in the rat cortex (Mezey et al., 2003) and on its key role in cell migration (Close et al., 2006), we further investigated the roles of Elongator in cerebral corticogenesis, where this process is critical. Elp1 mRNA transcripts were detected across landmark developmental stages and throughout the rostrocaudal axis of the telencephalon (Figure S1A available online). Analyses of the presumptive cortex revealed that Elp1 was primarily (embryonic day 12.5 [E12.5]) expressed throughout the cortical wall (Figure 1A and Figure S1B) but later became (E14.5 and E18.5) restricted to the cortical plate (CP), the ventricular (VZ), and subventricular (SVZ) zones (Figures 1B and 1C and Figure S1B). Its expression was sharply downregulated in the intermediate zone (IZ) at E18.5, when most projection neurons terminate their migration to the CP and undergo terminal differentiation (Figure 1C and Figure S1B). Immunoblots of whole-cell extracts from microdissected E14.5 cortices or ganglionic eminences (GE) indicated that Elongator subunits (Elp1, Elp3, Elp4, and Elp5) were expressed in these structures (Figure 1D). Immunostainings performed on E14.5 brains showed that Elp1 was mainly expressed in the cytoplasm (Figure 1H) of IZ and CP (Figures 1E–1G) βIII-tubulin positive neurons (Tuj1$^+$, Figures 1J–1L). Calretinin-positive Cajal-Retzius cells located at the top of the cortex exhibited the strongest Elp1 expression level among cortical cells (Figures 1M–1O). Other Elongator subunits (Elp3, Elp4, and Elp5) were detected at E14.5 in all IZ and CP cells as cytoplasmic proteins (Figures 1P–1X′ and Figures S14B, S14H, and S14L). The overlapping expression of Elongator subunits in cortical progenitors suggests that they may assemble into a functional complex and regulate several aspects of their maturation into functional projection neurons.

Elp1 Regulates the Migration Rate of Projection Neurons into the Cerebral Cortex

Since the Elongator complex is dispensable for the survival (Figure S2), the proliferation, and the exit of the cell cycle of cortical progenitors (Figures S3G–S3L) and since most subunits of this complex are expressed in postmitotic regions of the developing cortex (Figures 1G, 1Q, 1T, and 1W), we examined whether its activity contributes to radial migration of projection neurons. So that this issue could be addressed, E14.5 mice were electroporated with control or Elp1 shRNA constructs (Figures S3A–S3F), followed 3 days later by analyses of cell position in the cortical wall of the developing somatosensory cortex (ssCx, Figure S6S) regionally divided into CP, IZ, and SVZ/VZ (Figure 2A). Elp1 silencing impaired radial migration (Figures 2D–2F) as it resulted in accumulation of electroporated cells in the VZ/SVZ (Figure 2B, 35.1% ± 3.5% for sh Elp1b and 39.6% ± 4.6% for sh Elp1a compared with 22.2% ± 1.9% for sh Ctrl) together with a reduced percentage of projection neurons in the CP compared to control experiments (Figure 2B, 14.5% ± 3.2% for sh Elp1b and 14.7% ± 1.6% for sh Elp1a compared with 26.7% ± 2.5% for sh Ctrl). Migration defects were obvious in the IZ at earlier time points (Figure S4A), led to impaired cell movement from VZ/SVZ to IZ as well as from IZ to CP (Figure S4B), and were not resulting from off-target activities (Figure S4C–S4E). Importantly, real-time analysis of cell migration in slice cultures from electroporated brains (Figure S5A and S5B) indicates that Elp1 regulates the speed of migration of bipolar and multipolar cortical cells (Movies S1 and S2). Although both cell types were migrating at expected rates in control conditions (Tabata and Nakajima, 2003), corresponding Elp1-depleted cells were moving approximately two times slower across the cortical wall (Figures 2C, Figures S5C–S5F, and Movies S3–S6). The radial glia scaffold along which cortical projection neurons migrate remained unperturbed (Figures S6A–S6F), indicating that Elp1 silencing specifically and cell-autonomously interfered with radial migration of projection neurons. Analyses conducted at postnatal day 2 (P2), an age by which targeted projection neurons have completed radial migration in control condition (Figure 2H), showed that the defect in migration was temporary as Elp1-depleted neurons finally reached their terminal destination (Figures 2G and 2I). Altogether, these observations indicate that Elp1 cell-autonomously delays the course of radial migration rather than permanently blocking it.

Defective Branching in Terminally Differentiating Projection Neurons Depleted for Elongator Subunits

Elp1 silencing affected the morphology but not the survival (Figure S7) of projection neurons in the CP, as evidenced by the absence of growing apical dendrite tree and leading processes harboring bulges (compare Figure S6H with Figures S6J and S6L). Although the shape of targeted cells located within the VZ and SVZ remained unchanged (data not shown), some neurons that were entering the lower IZ harbored highly twisted leading processes characterized by multiple bendings (compare Figure S6N with Figures S6P and S6R). Noticeable differences in process extensions of neurons silenced for Elp1 were also observed at low magnification in the cortex of P2 pups (Figures

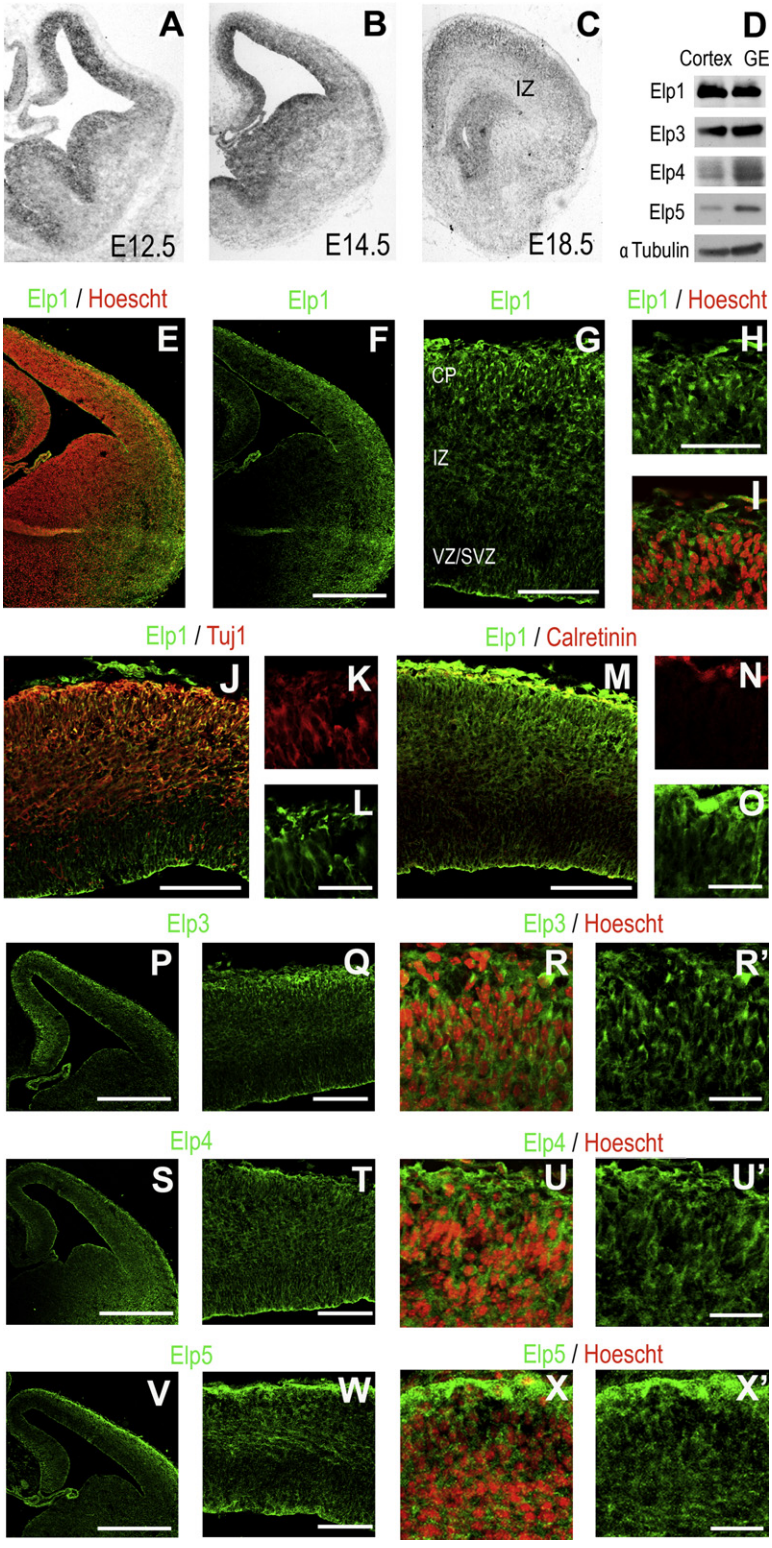

Figure 1. Elongator Subunits Are Expressed in the Developing Cerebral Cortex

(A–C) *Elp1* transcript distribution in frontal sections of the telencephalon at different developmental stages.

(D) Western blot analyses showing Elongator complex subunits in E16 cortices.

(E–O) Predominant expression of Elp1 in postmitotic regions of the telencephalon (E and F) as confirmed on a close-up picture of the dorsal cortex (G). Elp1 (green) is mostly confined to the cytoplasm of cortical neurons that are βIII-tubulin positive (J–L) (Elp1 in green, Tuj1 in red) and excluded from their nuclei (H and I) (Hoescht 33342 in red). Strongest staining for Elp1 (green) is observed in calretinin-expressing Cajal-Retzius cells (red) (M–O).

(P–R′) Elp3 protein expression pattern in the cortex (Hoescht 33342 in red, Elp3 in green).

(S–X′) Elp4 and Elp5 expression in postmitotic regions of the cortex (S, T, V, and W) with predominant cytoplasmic staining (U, U′, X, and X′) (Hoescht 33342 in red and Elp4 or Elp5 in green).

Scale bars represent 500 μm (F, P, S, and V), 100 μm (J, M, Q, T, and W), 75 μm (G), 50 μm (H), and 25 μm (L, O, R′, U′, and X′).

S6T–S6V) and prompted us to investigate whether Elongator regulates the branching of terminally differentiating projection neurons.

To address this issue, E14.5 embryos were electroporated ex vivo with shRNA vectors, dissociated, and cultured for 4 days. Elp1 silencing impaired the growth of both dendrites and axons but not the soma perimeter (Figures S8A–S8K). To further explore the role of Elp1 in neuronal branching in vivo, E14.5 embryos were electroporated and allowed to survive until P2. The morphology of differentiating projection neurons located in the ssCx (Figure 3A) was analyzed by confocal microscopy. The intensity of GFP expression was reduced in axonal projection from Elp1-depleted projection neurons compared to sh Ctrl-electroporated neurons (see arrows in Figures 3B–3D), suggesting growth defects of corticocortical tracts that are consistent with the in vitro results (Figures S8G–S8H). Confocal images projection of GFP expressing neurons randomly acquired along the ssCx (Figures 3E–3G″) were used to perform computer-assisted reconstruction of dendrite trees (Figures 3H–3J). Strikingly, while the average soma perimeter remained unchanged after Elp1 silencing (Figure 3K), the total dendrite length (Figure 3L) and branch numbers (Figure 3M) were reduced compared to the control. To assess the overall dendritic morphology of projection neurons, we calculated the dendritic complex index (DCI) (Lom and Cohen-Cory, 1999) and showed that Elp1 knockdown resulted in lower DCI values (Figure 3N, 308.1 ± 57.1 for sh Elp1a, 542.5 ± 82.6 for sh Elp1b compared with 835.1 ± 93.7 for sh Ctrl). Defects in dendritic branching were still noticeable in Elp1-depleted projection neurons at P17 when projection neurons were fully differentiated (Figure S9). To further establish the role of Elongator in dendritogenesis, we performed rescue experiments by expression of a Flag human ELP1 refractory to silencing by both sh Elp1a and sh Elp1b (Figure 4A, ELP1 FL). Coexpression of ELP1 with

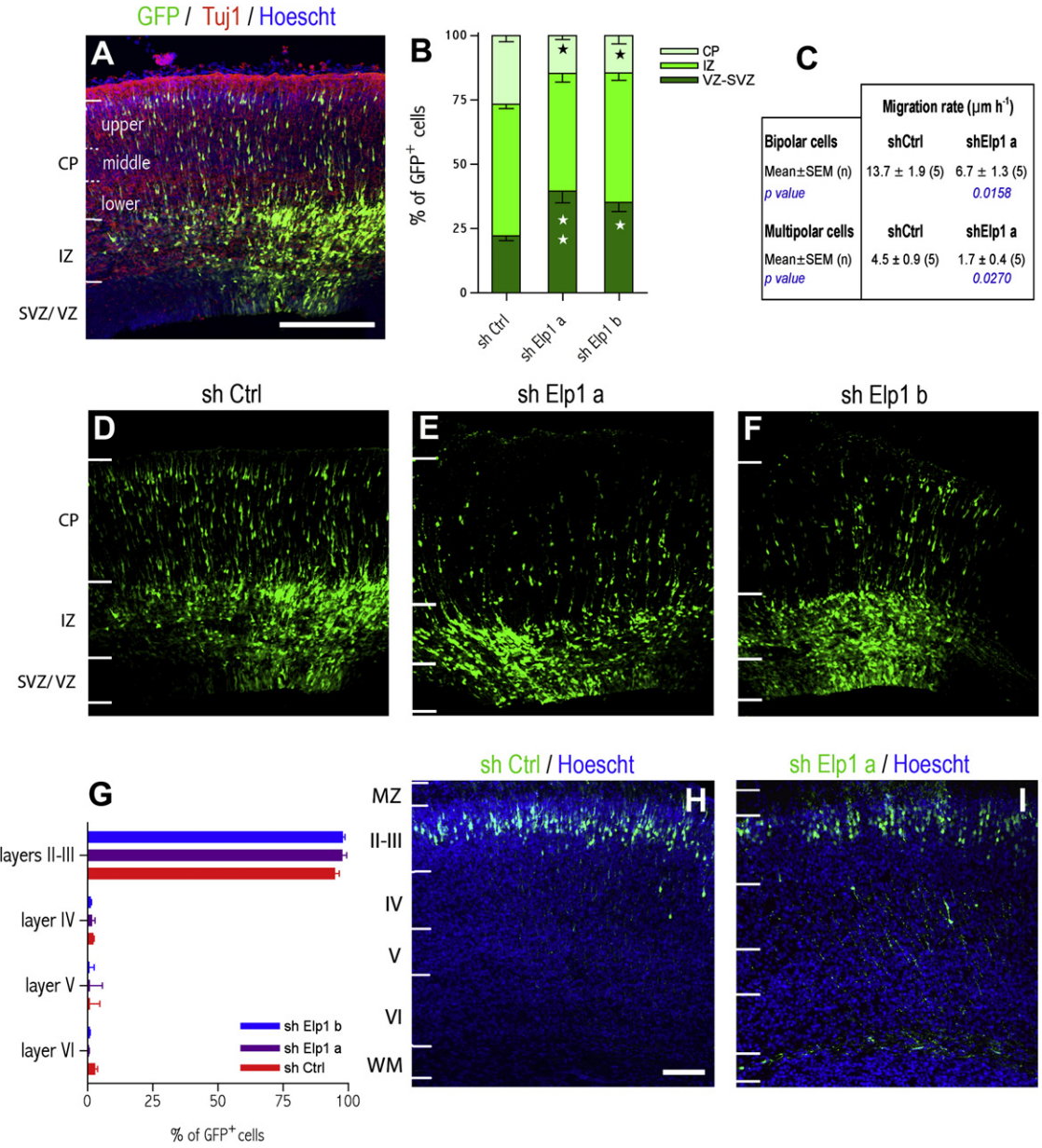

Figure 2. Acute Depletion of Elp1 Alters the Migration of Projection Neurons into the Cerebral Cortex

(A–F) Subdivision of the cortical wall into CP, IZ, and VZ/SVZ according to triple immunostainings (GFP, green; βIII-tubulin [Tuj1], red; Hoescht 33342, blue) (A). Distribution of GFP-positive cells is shown in E17.5 cortices, 3 days after electroporation (D–F). Percentages of electroporated cells that distributed in distinct cortical areas are shown ([B], n = 3–5 brains, mean ± SEM). The table shows the average migration rate of bipolar and multipolar cortical cells in brain slices electroporated with either shCtrl or shElp1a ([C], 50 and 69 cells recorded, respectively).

(G–I) Distribution of shRNA-electroporated cells at P2 (n = 3 brains, mean ± SEM). CP, cortical plate; IZ, intermediate zone; SVZ, subventricular zone; VZ, ventricular zone; MZ, marginal zone; and WM, white matter.

Scale bars represent 200 μm (A) and 150 μm (H).

either sh Elp1a (Figures 4D–4F) or shElp1b (data not shown) fully corrected the dendrite branching defects (Figure 4C). Interestingly, ELP1 was cytoplasmic (Figure 4G′), which suggests that Elongator regulates neuronal branching by targeting cytosolic components. The attempt to rescue branching defects with the truncated ELP1 found in patients suffering from FD (Figure 4A, ELP1 ΔC622) failed, likely because it was mildly expressed (Figure 4B, second panel from the top, compare lane 4 with lane 3). Surprisingly, although strongly expressed in the cytoplasm (Figure 4K′), ELP1 ΔC732 failed to rescue the branching defects seen upon Elp1 depletion (Figures 4C and 4H–4J), likely because of its inability to efficiently bind ELP3 in contrast to full-length ELP1 (Figure 4B, top panel, compare lane 3 with lane 5). Thus, these results suggest that a physical interaction between

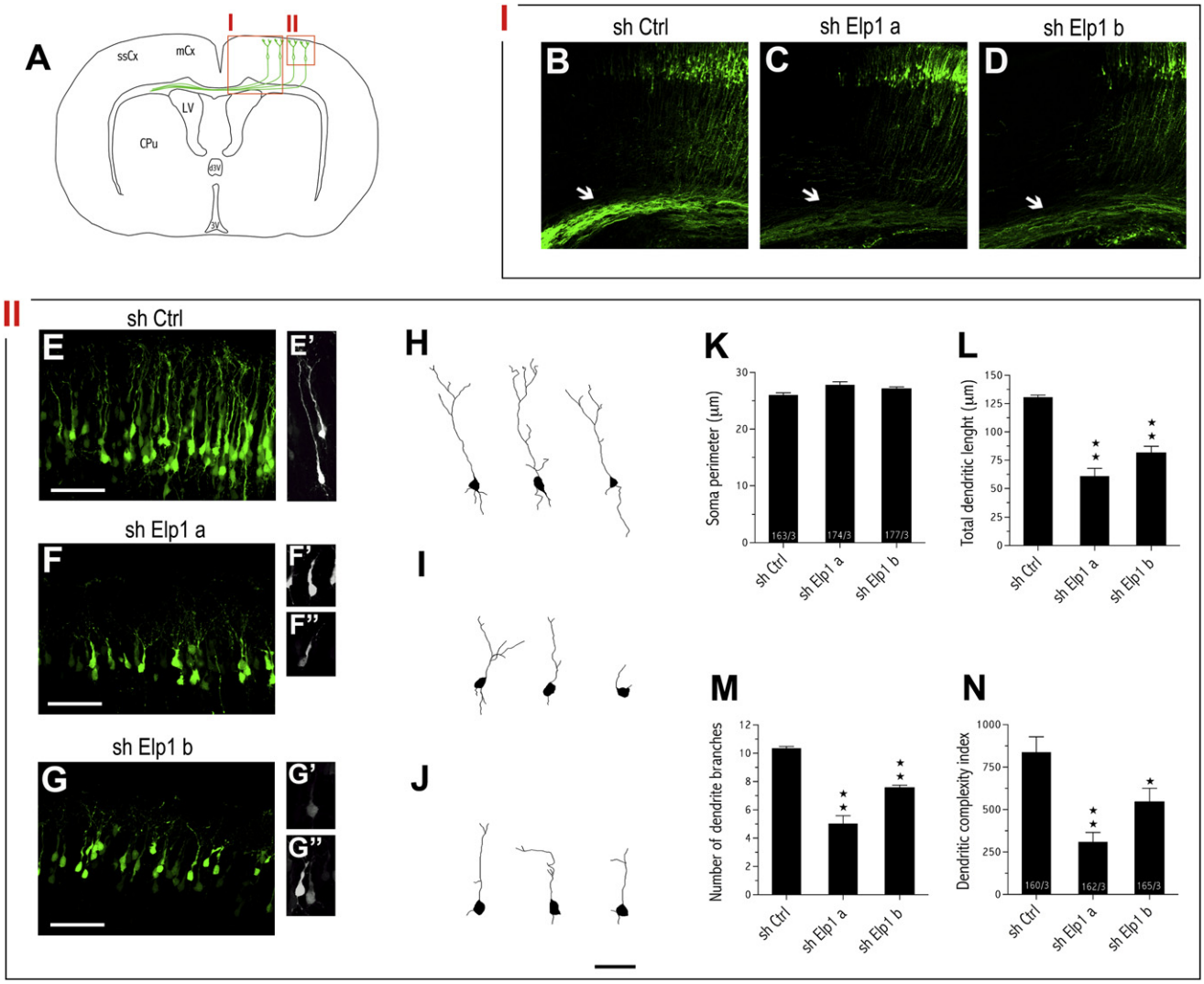

Figure 3. Defective Branching in Terminally Differentiating Projection Neurons Depleted for Elp1

(A) Drawing of a frontal section through an electroporated mouse brain illustrating the regions (boxed in red) where the axonal projections (I) or the dendrite tree (II) of transfected neurons (green) were analyzed at P2.

(B–D) Representative pictures of corticocortical axonal projections from electroporated neurons. The arrows point the reduction in GFP intensity of corticocortical axonal projections after Elp1 silencing (C and D) compared with control (B).

(E–G″) Representative electroporated neurons in the upper layers of P2 mouse cortex.

(H–J) Tracings of representative GFP-positive neurons for each condition. Axons are not represented.

(K–N) Soma perimeter of electroporated cortical neurons ([K], n = 3 brains, mean ± SEM; numbers in parentheses refer to both the total number of cells and the number of brains analyzed). Histograms illustrate the total dendritic length (L), the numbers of dendrite branches (M), and the dendritic complexity index ([N], DCI) of transfected cortical neurons (n = 3 brains, mean ± SEM). ssCx, somatosensory cortex; mCx, motor cortex; LV, lateral ventricle; CPu, caudate putamen; 3rd V, third ventricle.

Scale bars represent 50 μm (E–G) and 25 μm (H–J).

Elp1 and Elp3 is required for neuronal branching of postmigratory projection neurons and that the morphological defects observed upon Elp1 depletion may directly result from a lack of Elp3 activity. This hypothesis is indeed supported by the constitutive interaction of ELP3 with ELP1 at the endogenous level in all cell types investigated (HEK293, SK-N-BE and HT29 cells) (Figure S10). Accordingly, we found that the branching of Elp3-depleted projection neurons was reduced both in vitro (Figures S8L–S8U) and in vivo (Figures 4L–4O). Furthermore, Elp3-silenced projection neurons displayed defects in radial migration (Figures 4P–4R) comparable to those in Elp1-knockdown neurons (Figure 2E). Thus, these data suggest that Elp3 is required for radial migration and branching of cortical projection neurons, most likely as a partner of Elp1. As Elp3 is the only catalytic subunit of Elongator (Wittschieben et al., 1999) and is destabilized upon Elp1 depletion (Petrakis et al., 2004), our data suggest that Elp3 activity underlies the migration and branching of cortical projection neurons.

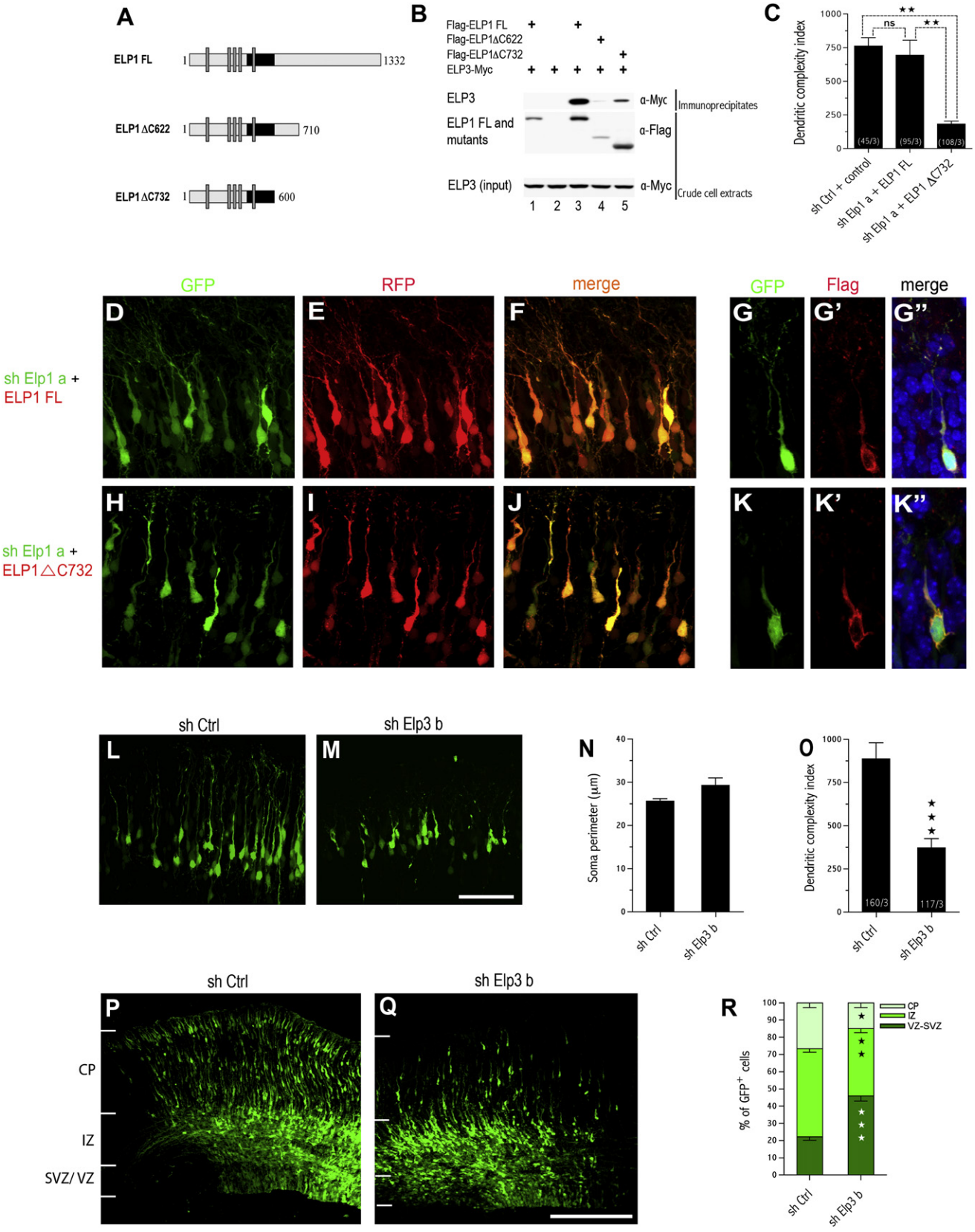
A
ELP1 FL
1
1332
ELP1 ΔC622
710
ELP1 ΔC732
600
B
Flag-ELP1 FL
Flag-ELP1ΔC622
Flag-ELP1ΔC732
ELP3-Myc
ELP3
α-Myc
Immunoprecipitates
ELP1 FL and mutants
α-Flag
ELP3 (input)
α-Myc
Crude cell extracts
1 2 3 4 5
C
Dendritic complexity index
ns
(45/3)
(95/3)
(108/3)
sh Ctrl + control
sh Elp1 a + ELP1 FL
sh Elp1 a + ELP1 ΔC732
GFP
RFP
merge
Flag
sh Elp1 a + ELP1 FL
sh Elp1 a + ELP1△C732
sh Ctrl
sh Elp3 b
Soma perimeter (μm)
160/3
117/3
CP
IZ
SVZ/ VZ
VZ-SVZ
% of GFP+ cells

Elongator Subunits Interact with the Microtubules and Are Required for Proper Acetylation of α-Tubulin

A variety of Elongator-deficient cell types showed impaired cell shape and motility, yet the mechanisms underlying this defect remained poorly characterized (Close et al., 2006). ELP1-depleted HT29 cells presented abnormal rounded shapes (Figures S11C and S11D), as well as major delays in cell spreading (Figure S12). Defective transcriptional elongation of genes coding for proteins involved in cell motility such as paxillin and gelsolin is not the only mechanism involved as they were correctly transcribed in ELP1-depleted SK-N-BE and HT29 cells (Figure S13), yet those cells did not spread properly (Close et al., 2006). We selected HT29 cells where ELP1 and ELP3 depletions through lentiviral shRNA infections are very efficient (Figure 5I). Endogenous ELP1 and ELP3 (Figures 5A and 5C) as well as the corresponding tagged proteins (Figures 5B and 5D) were mainly found in the cytoplasm, where they show a partial colocalization with α-tubulin and its acetylated form (Figures 5A″, 5B, 5C″, and 5D and Figures S11A and S11B). Those data suggest an association of Elongator with microtubules, as previously reported for the α-tubulin deacetylase HDAC6 (Hubbert et al., 2002; Zhang et al., 2003) (Figures S14M–S14P″). In support of this idea, nocodazole treatment, which collapses the microtubule network, randomized the cytosolic distribution of both HDAC6 (Figures S11E and S11F) and Elongator subunits (Figures S11G–S11J). Accordingly, we reasoned that a pool of both ELP1 and ELP3 could interact with polymerized α-tubulin. To address this issue, we purified microtubules from HEK293 cells and detected HDAC6 and also both ELP1 and ELP3 but not β-actin in the pellet fraction, which contains microtubules and microtubule-associated proteins (Figure 5E). This association was specific as both ELP1 and ELP3 presences in the pellet fraction were increased when GTP and Taxol, a microtubules stabilizer, were added (Figure 5E). In addition, we showed that ELP1 and ELP3 are part of a common complex with α-tubulin as evidenced by coimmunoprecipitation studies in HEK293 cells. Ectopically expressed ELP1 or ELP3 bound endogenous acetylated α-tubulin and α-tubulin (Figures 5F and 5G). As expected, ELP1 was also found in the anti-ELP3 immunoprecipitates, which suggests that acetylated α-tubulin is associated with the whole Elongator complex (Figure 5G). Importantly, HDAC6 (positive control) and also ELP3 associated with α-tubulin at the endogenous level in both HEK293 or neuroblastoma-derived SH-SY 5Y cells (Figure 5H).

We next investigated whether ELP1 or ELP3 silencing would impact α-tubulin acetylation (Gardiner et al., 2007). This cytoskeletal protein is acetylated on lysine 40 (Gaertig et al., 1995; Kozminski et al., 1993), a posttranscriptional modification required for the anchoring of molecular motors and thus critical for microtubule-based molecular transport (Dompierre et al., 2007; Reed et al., 2006). ELP1- or ELP3-depleted HT29 cells indeed showed lower levels of acetylated α-tubulin but not α-tubulin (Figure 5I and Figure S11D). These data suggest that Elongator regulates α-tubulin acetylation, a posttranscriptional modification likely required for dynamic cell shape remodeling and motility.

ELP3-Enriched Fraction Acetylates α-Tubulin

Elp3, which acetylates histone H3 and to a lesser extent histone H4, is essential for Elongator function in vivo (Wittschieben et al., 2000). Thus, we next explored whether Elongator directly acetylates α-tubulin. For that purpose, we expressed His-tagged Elp3 from a baculovirus in Sf9 insect cells and isolated a soluble fraction highly enriched in recombinant Elp3, as shown by western blot analyses (Figures 5J). HAT assays using Histone H3 as control demonstrated that this fraction was promoting H3 acetylation in a dose-dependant manner, almost as efficiently as a recombinant p300 (Figures 5K and 5L). Importantly, the Elp3-enriched fraction induced α-tubulin acetylation from purified microtubules (Figure 5M) but with a reduced efficiency, likely because this substrate was already massively acetylated, as seen by western blot (data not shown). Biochemical analyses of transfected HEK293 cells demonstrated that ELP3 expression counteracted HDAC6-mediated α-tubulin deacetylation in a dose-dependent manner and that its HAT domain was required as an ELP3 mutant (ELP3ΔHAT) in which the amino acid residue 529 was mutated (Y529A) failed to do so (Figure 5N and 5O).

Elp1 expression was also observed in the cytoplasm of cultivated cortical neurons, where it fully colocalized with either α-tubulin (Figures 6A–6A″) or its acetylated form (Figures 6B–6B″). Elp3 also showed a cytosolic expression overlapping with both α-tubulin (Figures 6C–6C″) and acetylated α-tubulin (Figures 6D–6D″). Of note, although Elp1 was almost exclusively cytoplasmic, a nuclear staining for Elp3 was noticeable in some neurons (see Figure 6C). As for HEK293 cells, we purified microtubules from E16 cerebral cortices and confirmed the enrichment of Elp1 after taxol treatment (Figure 6E). So that α-tubulin acetylation in Elongator-deficient cortical projection neurons

Figure 4. Elongator Controls Radial Migration and Branching of Cortical Projection Neurons via Elp3

(A) Full-length (ELP1 FL) or truncated (ELP1 ΔC622 and ELP1 ΔC732) human ELP1 protein.

(B) Cell extracts from HEK293 cells transfected with the indicated constructs and immunoprecipitated with anti-HA (negative control, lane 1) or anti-Flag antibodies (lanes 2 to 5) followed by an anti-Myc western blot (top panel). Crude cell extracts were also subjected to anti-Flag and anti-Myc western blots (bottom panels).

(C–K″) DCI of electroporated cortical projection neurons in P2 mices (C). Immunolabelings show the expression of GFP and RFP in P2 projections neurons electroporated at E14.5 with specific plasmid combinations, as indicated (D–K″). Flag epitopes were immunodetected in the cytosolic compartment of transfected neurons (G–G″ and K–K″) (GFP in green, Flag in red, and Hoescht 33342 in blue).

(L–R) Morphological analysis of in utero-electroporated neurons in the ssCx of P2 mouse brains. Representative GFP-positive neurons electroporated with either sh Ctrl (L) or sh Elp3b (M). Histograms show the average soma perimeter of electroporated cortical neurons ([N], n = 3 brains, mean ± SEM) and values for their DCI ([O], n = 3 brains, mean ± SEM; numbers in parentheses refer to both the total number of cells and brains analyzed). Immunolabelings show the distribution of electroporated cells (green) with sh Ctrl (P) or sh Elp3b (Q) in E17.5 cortices, 3 days after electroporation. The histogram shows the percentage of electroporated cells in all compartment of the cortex ([R], n = 5–7 brains, mean ± SEM).

Scale bars represent 50 μm (L and M) and 200 μm (P and Q).

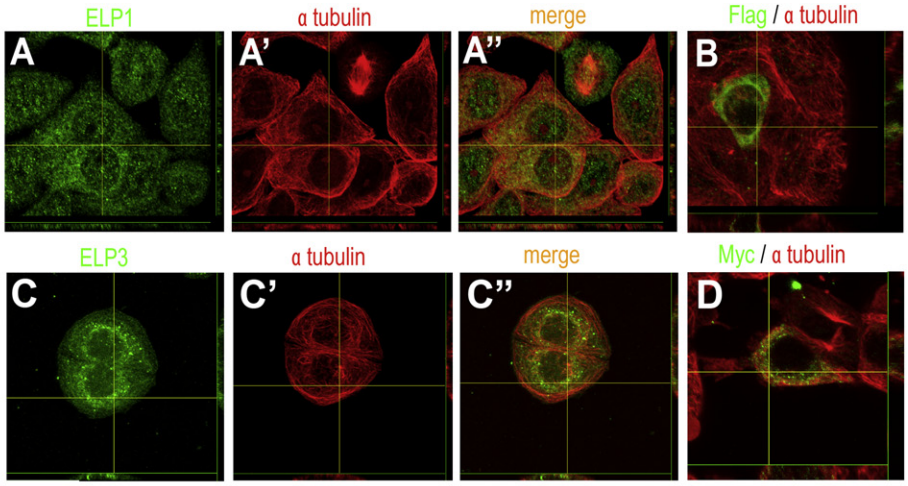
ELP1
α tubulin
merge
Flag / α tubulin
A
A'
A''
B
ELP3
α tubulin
merge
Myc / α tubulin
C
C'
C''
D

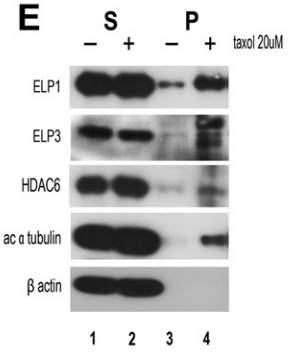
E
S
P
taxol 20uM
ELP1
ELP3
HDAC6
ac α tubulin
β actin
1 2 3 4

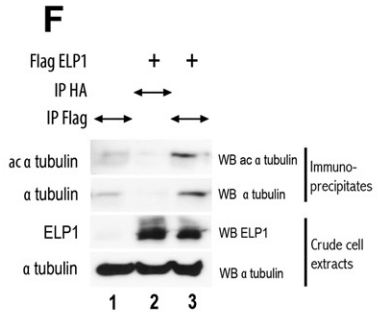
F
Flag ELP1
IP HA
IP Flag
ac α tubulin
α tubulin
ELP1
α tubulin
WB ac α tubulin
WB α tubulin
WB ELP1
WB α tubulin
Immuno-precipitates
Crude cell extracts
1 2 3

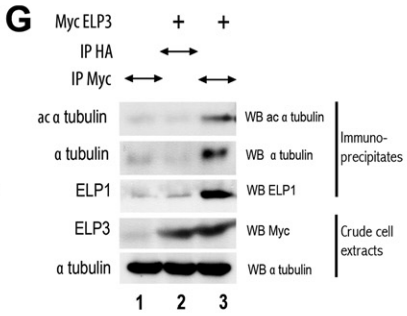
G
Myc ELP3
IP HA
IP Myc
ac α tubulin
α tubulin
ELP1
ELP3
α tubulin
WB ac α tubulin
WB α tubulin
WB ELP1
WB Myc
WB α tubulin
Immuno-precipitates
Crude cell extracts
1 2 3

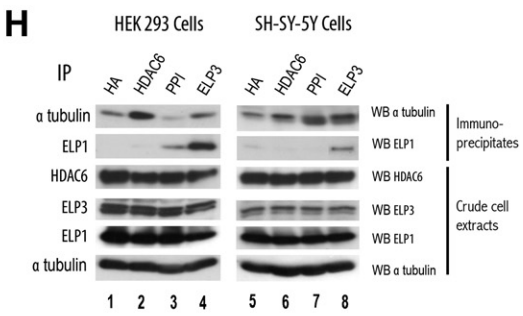
H
HEK 293 Cells
SH-SY-5Y Cells
IP
HA
HDAC6
PPI
ELP3
α tubulin
ELP1
HDAC6
ELP3
ELP1
α tubulin
WB α tubulin
WB ELP1
WB HDAC6
WB ELP3
WB ELP1
WB α tubulin
Immuno-precipitates
Crude cell extracts
1 2 3 4 5 6 7 8

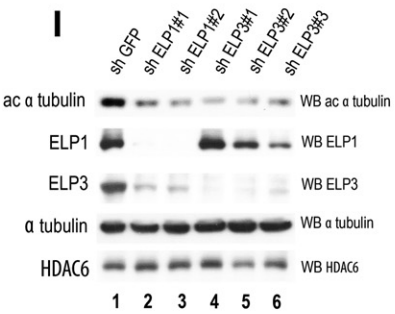
I
sh GFP
sh ELP1#1
sh ELP1#2
sh ELP3#1
sh ELP3#2
sh ELP3#3
ac α tubulin
ELP1
ELP3
α tubulin
HDAC6
WB ac α tubulin
WB ELP1
WB ELP3
WB α tubulin
WB HDAC6
1 2 3 4 5 6

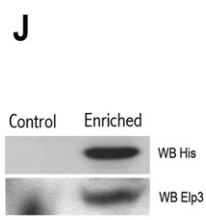
J
Control
Enriched
WB His
WB Elp3

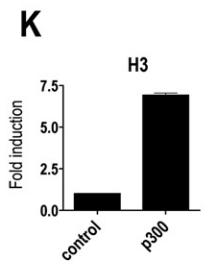
K
H3
Fold induction
7.5
5.0
2.5
0.0
control
p300

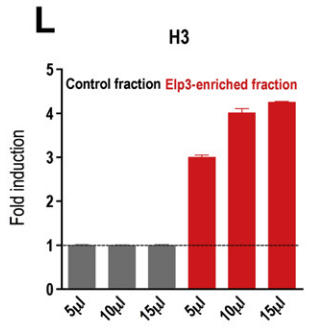
L
H3
Control fraction
Elp3-enriched fraction
Fold induction
5
4
3
2
1
0
5μl
10μl
15μl
5μl
10μl
15μl

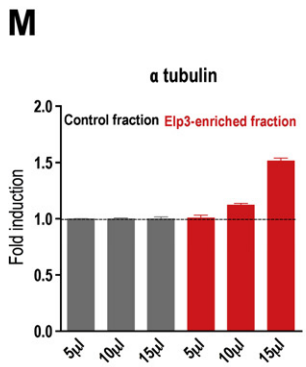
M
α tubulin
Control fraction
Elp3-enriched fraction
Fold induction
2.0
1.5
1.0
0.5
0.0
5μl
10μl
15μl
5μl
10μl
15μl

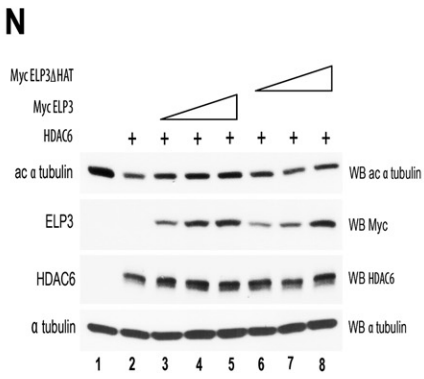
N
Myc ELP3ΔHAT
Myc ELP3
HDAC6
ac α tubulin
ELP3
HDAC6
α tubulin
WB ac α tubulin
WB Myc
WB HDAC6
WB α tubulin
1 2 3 4 5 6 7 8

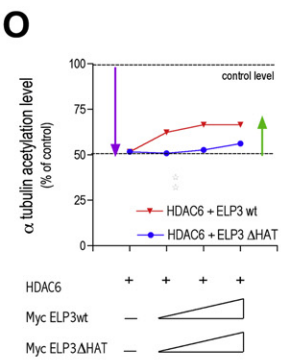
O
α tubulin acetylation level
(% of control)
100
75
50
25
0
control level
HDAC6 + ELP3 wt
HDAC6 + ELP3 ΔHAT
HDAC6
Myc ELP3wt
Myc ELP3ΔHAT

could be assessed, E14 cortical progenitors were electroporated ex vivo with sh Elp1a or sh Elp3b and cultured for 4 days to allow neuronal differentiation. Although neurons experienced branching defects (Figure S8), acetylated α-tubulin levels were often strongly reduced (Figures 6F–6H′). Interestingly, Elp1 silencing did not affect the expression level or the activation of Pak1, a key molecule acting downstream of the Rac proteins in neuronal dendritogenesis (Hayashi et al., 2002) (Figure S15A). In addition, abundant actin filaments were observed in the leading processes of both control and Elp1-silenced differentiating cortical projection neurons in vivo, suggesting that Elongator does not primarily regulate cell migration and branching through extensive remodeling of the actin cytoskeleton (Figures S15B–S15E). Thus, our data demonstrate that Elongator interacts with and controls α-tubulin acetylation in various cell types, including cortical projection neurons, and suggest that Elp3 directly acetylates this substrate.

α-Tubulin Acetylation Promotes Radial Migration and Branching of Cortical Projection Neurons

To further explore the link between Elongator activity, α-tubulin acetylation, and corticogenesis, we determined the impact of a forced reduction in α-tubulin acetylation on the migration and differentiation of projection neurons by using a dominant-negative α-tubulin form that cannot be acetylated (α-tubulin K40A) (Dompierre et al., 2007) (Figure S16). We showed that expression of α-tubulin K40A (Figures 7B and 7C) but not wild-type (WT) α-tubulin (Figure 7A) impaired radial migration to a similar extent as was seen in Elp1/Elp3 knockdown experiments (Figures 2B and 4R). Of note, the expression of both constructs sometimes led to morphological abnormalities, irrespective of cell location in the cortical wall (data not shown). Importantly, the electroporation of the α-tubulin K40A mutant in Elp1-depleted versus control neurons did not potentiate but led to similar migration defects (Figures 7D and 7E). Moreover, when analyzed later in the ssCx of P2 mice (Figures 7F, 7G, 7I, and 7J), neurons expressing α-tubulin K40A showed a reduction of DCI compared with the control (Figure 7K, 504.6 ± 53.8 for α-tubulin K40A and 854.2 ± 44.3 for the control) although the soma perimeter remained unaffected (Figure 7H). Elp3 overexpression counteracted HDAC6-mediated α-tubulin deacetylation (Figure 5N), which suggests that Elongator may reverse HDAC6 function. We therefore reasoned that increased α-tubulin acetylation after HDAC6 inhibition would restore, at least partially, the branching defects seen upon Elp3 depletion in cortical neurons. The HDAC6 deacetylase domain-selective inhibitor tubacin but not its inactive carboxylate analog niltubacin (Haggarty et al., 2003) restored acetylated α-tubulin levels in ELP1- and ELP3-depleted HT29 cells (Figure S17A). Importantly, addition of tubacin but not niltubacin to cultivated brains slices rescued the branching defects of Elp3-depleted cortical neurons (Figures S17B and S17C). As we showed that Elongator regulates α-tubulin acetylation through Elp3 activity, these results suggest that this process is an important mechanism by which Elongator regulates the migration and branching of projection neurons in the developing cerebral cortex.

DISCUSSION

The characterization of the molecular controls driving the maturation of cortical progenitors into projection neurons is important to the understanding of how cortical architecture, connectivity, and functions emerge during development. We show here that Elongator regulates corticogenesis because an acute disruption of its activity in dorsal progenitors results in radial migration delays and defective terminal branching of projection neurons that come with a reduction in α-tubulin acetylation. Importantly, this complex interacts with the microtubule cytoskeleton, where Elp3 may directly acetylate α-tubulin, a posttranslational modification known to regulate the intracellular trafficking that is critical for cell shape remodeling during migration and terminal branching.

Role of Elongator during Neurogenesis in the Cerebral Cortex

We previously hypothesized that some pathological aspects of FD result from cell motility defects of neuronal cells, and such

Figure 5. Elp3 Promotes the Acetylation of α-Tubulin

(A–D) ELP1 (A), ELP3 (C), α-tubulin (A′ and C′) expression in HT29. Immunolabelings show a partial cytosolic colocalization (yellow) of α-tubulin (red) with ELP1 (green, [A″]) or with ELP3 (green, [C″]). Immunolabelings show a partial colocalization of α-tubulin (red) with Flag ELP1 (green, [B]) or with Myc ELP3 (green, [D]).

(E) Microtubules purified from HEK293 cell extracts with (lanes 2 and 4) or without Taxol and GTP. Proteins present in the pellet (P, lanes 3 and 4) and in the supernatant fractions (S, lanes 1 and 2) were analyzed by western blot with anti-ELP1, anti-ELP3, anti-HDAC6, anti-acetylated α-tubulin, and anti-β-actin antibodies, as indicated.

(F and G) HEK293 cells were transfected with the indicated expression plasmids, and anti-Flag (F), anti-Myc (G), or anti-HA (negative control) immunoprecipitates were subjected to anti-acetylated α-tubulin, anti-α-tubulin ([F] and [G], top panels), or anti-ELP1 ([G], third panel from the top) western blot analysis. Anti-ELP1, anti-Myc (G), and anti-α-tubulin western blots performed on crude cell extracts as indicated.

(H) Cell extracts from HEK293 or SH-SY-5Y cells were subjected to immunoprecipitations with the indicated antibodies followed by anti-α-tubulin or anti-ELP1 western blots (top and second panel from the top, respectively). Cell extracts were subjected to anti-α-tubulin, anti-ELP1, anti-ELP3, or anti-HDAC6 western analyses as well (bottom panels).

(I) Cell extracts from HT29 cells infected with the various lentiviral pLL3.7 shRNA targeting vectors subjected to anti-acetylated α-tubulin, anti-ELP1, anti-ELP3, anti-α-tubulin, and anti-HDAC6 western blot analysis as indicated.

(J) Purified His-Elp3-enriched (enriched) and nonenriched (control) fractions were subjected to anti-His or anti-Elp3 western blots to detect recombinant Elp3 expression.

(K–M) HAT assays using Histone H3 (K and L) or α-tubulin (M) as substrate and either a control or the Elp3-enriched fractions. Recombinant p300 was used as positive control (K).

(N–O) Wild-type but not a HAT-defective Elp3 mutant partially restores the levels of acetylated α-tubulin in HDAC6-overexpressing HEK293 cells. Cell extracts from HEK293 cells transfected with similar or increased amounts of the indicated expression plasmids were subjected to anti-acetylated α-tubulin, anti-ELP3, anti-HDAC6, and anti-α-tubulin western analysis (N). The ratio of acetylated versus α-tubulin levels is plotted and compared to the one obtained in control HEK293 cells ([O], set to 100%).

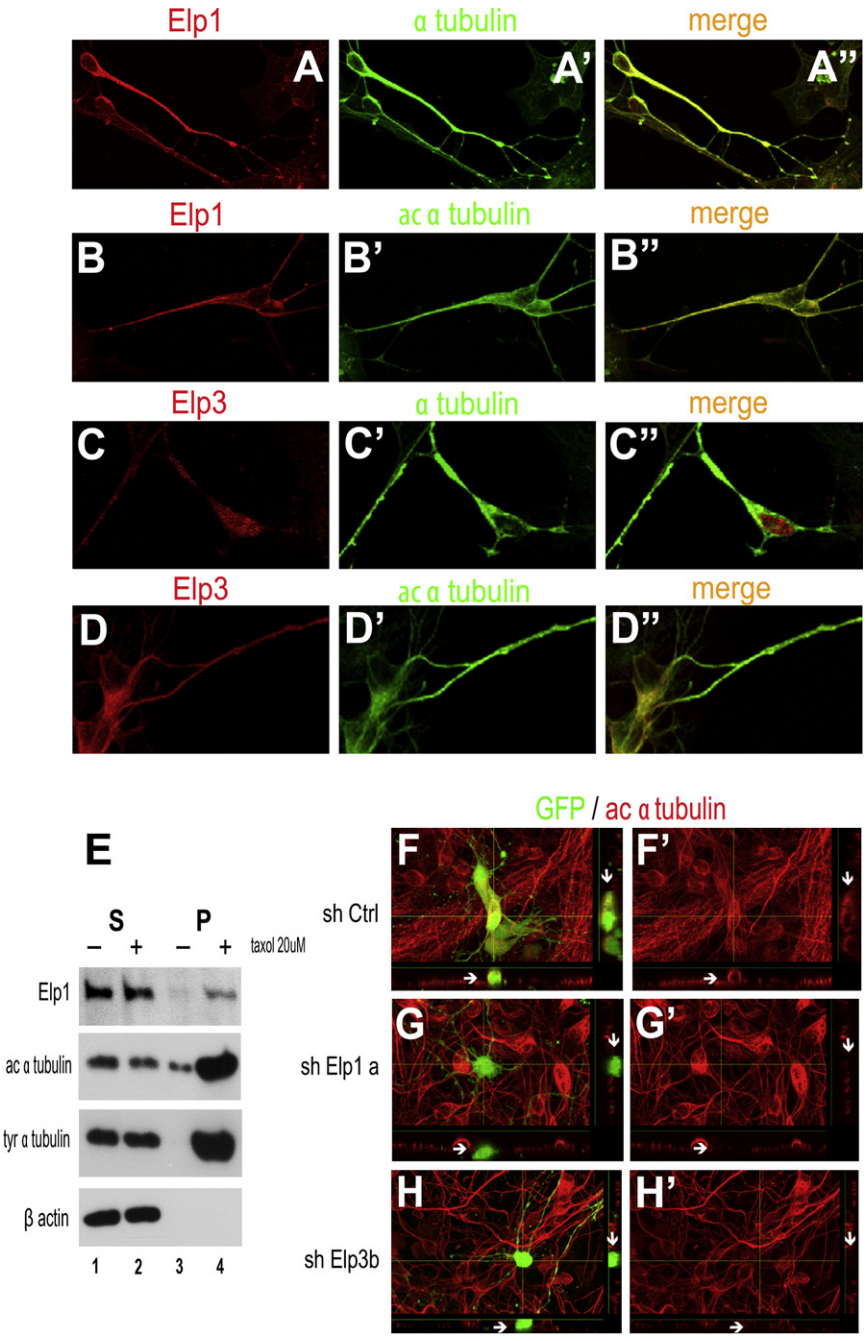

Figure 6. Elongator-Deficient Cortical Neurons Exhibit Reduced Expression of Acetylated α-Tubulin

(A–D″) Partial coexpression of Elp1 ([A] and [B], in red) with α-tubulin ([A′] in green) and acetylated α-tubulin ([B′], in green) as shown in E16 cortical neurons cultured for 4 days (A″ and B″). Similar observations were made for Elp3 (C–D″).

(E) Purified microtubules from embryonic cortical neurons extracts with (lanes 2 and 4) or without Taxol and GTP. The proteins present in the pellet (P, lanes 3 and 4) and in the supernatant fractions (S, lanes 1 and 2) were analyzed by western blot with the anti-ELP1, anti-acetylated α-tubulin, anti-tyrosinated α-tubulin, and anti-β-actin antibodies as indicated.

(F–H′) Acetylated α-tubulin in (red) expression levels in embryonic cortical neurons electroporated ex vivo at E14.5 with shRNA vectors (green) after 4 days of culture.

a conclusion was also recently drawn by others (Close et al., 2006; Johansen et al., 2008). We now provide evidence for a key role of Elongator in neuronal migration and highlight how critical is α-tubulin acetylation for this process to occur. Our data define Elongator as a molecular determinant in radial migration of projection neurons and establish a functional link between this complex and the microtubule network. Complex dynamic regulations of the cytoskeleton of neurons underlie distinct phases of migration in the cortex (LoTurco and Bai, 2006), and defects in the cytoskeletal machinery often underlie neurodevelopmental disorders characterized by impaired radial migration and placement in the neocortex (Marin and Rubenstein, 2003). One aspect of radial migration is the dynamic adaptation of the microtubule network as some mutations in genes such as *Lis1*, *Dcx*, and *Tuba1*, which regulate the microtubule cytoskeleton, cause lissencephaly in humans (Gleeson et al., 1998; Keays et al., 2007; Reiner et al., 1993). Although we suggest that Elongator promotes radial migration through α-tubulin acetylation, this could not be the only mechanism by which Elongator regulates cell migration in the cortex as ELP1 is also associated with filamin A in HEK293 cells (Johansen et al., 2008). This structural protein drives cell migration through reorganization of the actin cytoskeleton at the leading edge and contributes to the dynamic shape remodeling of cortical neurons that enter the IZ during radial migration (Nagano et al., 2004). However, delays in radial migration upon Elongator deficiency are more likely to result from a global reduction in α-tubulin acetylation rather than from a loss of function of filamin A as migratory defects were not exclusively affecting cell transition from SVZ to IZ (Nagano et al., 2004) or promoting the formation of periventricular nodular heterotopia (Fox et al., 1998). In addition, lowering α-tubulin acetylation levels in microtubules through expression of α-tubulin K40A recapitulated the migratory defects induced by Elp1/Elp3 silencing. Furthermore, the reduced acetylated α-tubulin levels seen upon Elongator deficiency suggest that this complex does not exclusively regulate cell motility via the transcriptional elongation of key genes coding for proteins involved in cell migration, as the identity of these genes is highly cell-specific (Close et al., 2006).

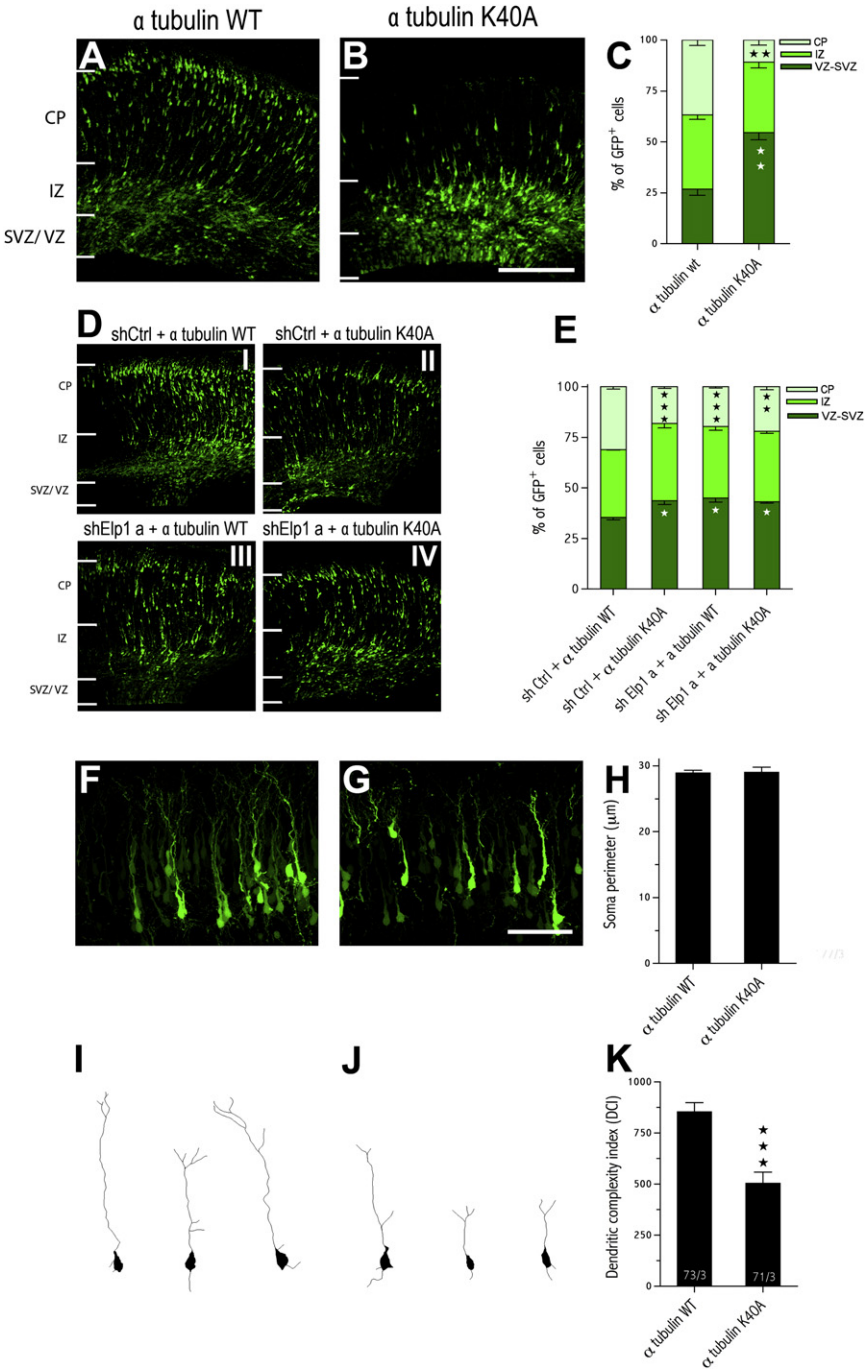

Figure 7. α-Tubulin Acetylation Underlies Radial Migration and Branching of Cortical Projection Neurons

(A–C) Radial migration in E17.5 cortices electroporated with α-tubulin WT (A) or α-tubulin K40A (B) together with reporter vectors (GFP, green). The histogram shows the percentage of GFP-positive cells migrating in distinct compartments of the cortex 3 days after electroporation ([C], n = 3 brains, mean ± SEM).

(D and E) Immunostainings showing GFP cells (green) in the cortex of E17.5 embryos electroporated with various plasmid combinations, as indicated ([D], I–IV). The histogram shows the distribution of the corresponding cells across the cortical wall ([E], n = 3 brains, mean ± SEM).

(F and G) Representative neurons overexpressing α-tubulin (F) or α-tubulin K40A (G) in P2 cortices.

(I and J) Tracings of 2D projection of representative GFP-positive neurons for each condition. Axons are not represented.

(H and K) Average soma perimeter of electroporated cortical neurons ([H], n = 3 brains, mean ± SEM) and DCI values ([K], n = 3 brains, mean ± SEM; numbers in parentheses refer to both the total number of cells and brains analyzed).

Scale bars represent 200 μm (B) and 50 μm (G).

The differentiation of projection neurons also critically depends on Elongator activity as the silencing of its scaffold (Elp1) or catalytic (Elp3) subunits resulted in branching defects. Although a reduction in acetylated α-tubulin was observed in Elongator-deficient projection neurons, no gross defects of the actin cytoskeleton were noticed. In addition, a forced reduction in α-tubulin acetylation equally impaired the branching of projection neurons and suggested that this posttranslational modification underlies cell shape remodeling and processes extension during differentiation. Furthermore, global defects in neuronal branching upon Elp1 silencing do not likely arise from delays in radial migration as we show that when neuronal branching and radial migration are uncoupled in vitro, Elongator deficiency still impairs neuronal branching although radial migration does not take place.

Suppression or mutation of the cytoskeletal regulator Nck-associated protein 1 (Nap1) leads to comparable branching defects in cortical neurons which, in addition, show reduced level of acetylated α-tubulin (Yokota et al., 2007). Since the cortices of P2 mice did not exhibit apparent neuron positioning defects, the authors suggested that Nap1 was not regulating radial migration. However, since we have uncovered delays in neuronal migration upon Elp1 depletion at earlier stages, it would be interesting to investigate the migration of Nap1-depleted cells at these embryonic stages. The relationship between α-tubulin acetylation, neuron migration, and branching is not yet clear but could rely on intracellular trafficking as α-tubulin acetylation is known to increase binding of motor proteins that regulate bidirectional molecular transport in axons and dendrites (Dompierre et al., 2007; Reed et al., 2006). Such posttranslational modification may underlie the transport of cytoskeleton elements (Roy et al., 2000) and/or proteins that are required during migration or that regulate the growth and maturation of axons or dendrites in cortical neurons

(Dajas-Bailador et al., 2008; Gomes et al., 2006). Such mechanisms would also impact local supply of ATP through transport of mitochondria in extending processes (Fujita et al., 2007). Our data are thus extending the biological roles played by Elongator as this complex is not only essential for the development and maintenance of sensory and autonomic neurons but is also required for the differentiation of projection neurons in the cortex, a critical step in its functional wiring.

Acetylation of Multiple Substrates May Underlie the Vast Arrays of Elongator Functions

Key roles of Elongator in transcriptional elongation, tRNA modifications, and exocytosis have been reported, yet the molecular mechanisms underlying these pathways remain poorly characterized (Svejstrup, 2007). Our data support the hypothesis that Elongator may fulfill those functions through acetylation of multiple substrates by Elp3 in distinct cell compartments. This possibility may help to solve the controversy surrounding the biological roles played by Elongator. Indeed, this complex acetylates histone H3 in the nucleus to promote transcript elongation and also targets cytoplasmic proteins such as α-tubulin and other unknown substrates. In support of this hypothesis, SIRT2, a mainly cytoplasmic deacetylase, targets α-tubulin in this cell compartment but also moves into the nucleus once phosphorylated by cyclin-dependent kinases in the G_2/M phase of the cell cycle in order to target histone H4 (North and Verdin, 2007; Vaquero et al., 2006). It is thus tempting to speculate that Elp3 localization and activity may also be regulated by posttranscriptional modifications, a mechanism that would explain how substrates located in distinct cell compartments are targeted by this acetylase. Whereas HDAC6 and SIRT2 deacetylate α-tubulin (Hubbert et al., 2002; North et al., 2003; Zhang et al., 2003), the enzymes responsible for α-tubulin acetylation remain unidentified. We show here that a purified Elp3-enriched fraction promotes α-tubulin acetylation in vitro and that Elp3, but not a HAT-defective Elp3 mutant, counteracts the HDAC6-mediated α-tubulin deacetylation in HEK293 cells. Altogether, these data strongly suggest that Elp3 directly acetylates α-tubulin in microtubules and are further supported by the fact that Elongator is mainly found in the cytoplasm and in purified microtubules, partially colocalizes and binds α-tubulin at the endogenous level, as reported for the α-tubulin deacetylases HDAC6 and SIRT2 (Hubbert et al., 2002; North et al., 2003; Zhang et al., 2003). Elongator may indeed target multiple uncharacterized substrates in the cytoplasm where a variety of proteins are acetylated (Kim et al., 2006).

In conclusion, we have identified Elongator as a key regulator of cerebral cortical development. We also provide evidence that Elongator binds to microtubules and that Elp3 promotes α-tubulin acetylation, a mechanism by which this complex may regulate the migration and differentiation of multiple cell types, including projection neurons.

EXPERIMENTAL PROCEDURES

Animals

Time-pregnant NMRI females (Harlan Netherlands, Horst, Netherlands) were housed under standard conditions and were treated according to the guidelines of the Belgian Ministry of Agriculture in agreement with European community Laboratory Animal Care and Use Regulations (86/609/CEE, Journal Official des Communautés Européennes number L358, 18 December 1986).

Tissue Processing

Embryonic brains were dissected in 0.1 M phosphate-buffered saline (PBS) (pH 7.4) and were fixed at 4°C in 4% paraformaldehyde (PFA) for 20 min (E12.5) to 1 hr (E14.5) (for immunohistochemistry) or overnight (for RNA in situ hybridization). P2 and P17 brains were dissected from anesthetized pups subjected to intracardial perfusion of 0.9% NaCl, followed by 4% PFA in 0.1 M NaH_2PO_4. Then brains were postfixed for 1.5–3.0 hr in 4% PFA. Fixed samples were cryoprotected overnight in 20% sucrose in PBS at 4°C, embedded in OCT Compound (VWR International, Leuven, Belgium), and sectioned (12–18 μm) onto slides (SuperFrost Plus, VWR International) with a cryostat.

Cell Cultures

Primary cortical neuron cultures were prepared from electroporated E14.5 or nonelectroporated E16.5 mouse cortices pooled into eppendorf tubes, incubated with Earl's Balanced Salt Solution (EBSS) (Invitrogen, Paisley, UK) containing 0.25% trypsin, 0.01% DNase, 1 mM $CaCl_2$, and 1 mM $MgCl_2$ for 20 min at 37°C and triturated with fire-polished Pasteur pipettes in Dulbecco's modified Eagle's medium (DMEM) supplemented with 1% glutamine, 10% fetal bovine serum (FBS), 1% penicillin-streptomycin, 6 g/l of glucose, and N2 Supplement. Dissociated cortical cells were seeded at a density of 50,000 cells per well onto polyornithin and laminin-coated (GIBCO) glass coverslips. Cells were cultured for 4 days in the same medium in humidified incubator at 37°C under 5% CO_2 atmosphere. SK-N-BE, HEK293, and HT29 cells were maintained as described (Close et al., 2006), whereas the HEK293FT cells were cultured in DMEM supplemented with 1% glutamine, 10% FBS, 1% antibiotics, and 500 μg/ml G418.

RNA In Situ Hybridization and Immunostainings

Nonradioactive RNA in situ hybridizations on frozen sections of brains were performed with digoxigenin-labeled sense and antisense riboprobes as described previously (Cau et al., 1997) with minor modifications. A 1 kb fragment of Elp1 was PCR cloned into pCR2.1-TOPO (Invitrogen) to generate both sense and antisense probes for human ELP1 (accession number NM_003640). Immunolabelings were performed as described in the Supplemental Experimental Procedures.

In Utero Electroporation

In utero electroporation, cell counting, and statistics were performed as described previously (Nguyen et al., 2006) with minor modifications, as explained in the Supplemental Experimental Procedures.

SUPPLEMENTAL DATA

Supplemental Data include Supplemental Experimental Procedures, 17 figures, one table, and six movies and can be found with this article online at http://www.cell.com/supplemental/S0092-8674(08)01518-3.

ACKNOWLEDGMENTS

The authors thank J.Q. Svejstrup, A. Goffinet, and A. Besson for critical reading of the manuscript, P. Gengoux and P. Leprince for technical assistance, and L. van Parijs, M. Vermeren, F. Saudou, and S.L. Schreiber for providing reagents. L.N., A.C., S.R., and B.M. are Postdoctoral Researcher, Research Associate, and Senior Research Associate, respectively, from the Belgian National Funds for Scientific Research (FNRS). C.C, M.G., and I.C. are TELEVIE Research Assistants, and M.-L.V. is a research fellow of the Fonds pour la formation à la Recherche dans l'Industrie et dans l'Agriculture (FRIA). This work was supported by grants from the FNRS, TELEVIE, the Belgian Federation against Cancer, the Concerted Research Action Program (04/09-323, University of Liege), the Inter-University Attraction Pole 6/12 (Federal

Ministry of Science), the Centre Anti-Cancéreux, the Fonds Léon Fredericq, and the Fondation Médicale Reine Elisabeth.

Received: May 8, 2008
Revised: September 12, 2008
Accepted: November 25, 2008
Published online: January 29, 2009

REFERENCES

Anderson, S.L., Coli, R., Daly, I.W., Kichula, E.A., Rork, M.J., Volpi, S.A., Ekstein, J., and Rubin, B.Y. (2001). Familial dysautonomia is caused by mutations of the IKAP gene. Am. J. Hum. Genet. *68*, 753–758.

Axelrod, F.B. (2004). Familial dysautonomia. Muscle Nerve *29*, 352–363.

Cau, E., Gradwohl, G., Fode, C., and Guillemot, F. (1997). Mash1 activates a cascade of bHLH regulators in olfactory neuron progenitors. Development *124*, 1611–1621.

Close, P., Hawkes, N., Cornez, I., Creppe, C., Lambert, C.A., Rogister, B., Siebenlist, U., Merville, M.P., Slaugenhaupt, S.A., Bours, V., et al. (2006). Transcription impairment and cell migration defects in elongator-depleted cells: implication for familial dysautonomia. Mol. Cell *22*, 521–531.

da Silva, J.S., and Dotti, C.G. (2002). Breaking the neuronal sphere: regulation of the actin cytoskeleton in neuritogenesis. Nat. Rev. Neurosci. *3*, 694–704.

Dajas-Bailador, F., Jones, E.V., and Whitmarsh, A.J. (2008). The JIP1 scaffold protein regulates axonal development in cortical neurons. Curr. Biol. *18*, 221–226.

Dompierre, J.P., Godin, J.D., Charrin, B.C., Cordelieres, F.P., King, S.J., Humbert, S., and Saudou, F. (2007). Histone deacetylase 6 inhibition compensates for the transport deficit in Huntington's disease by increasing tubulin acetylation. J. Neurosci. *27*, 3571–3583.

Esberg, A., Huang, B., Johansson, M.J., and Bystrom, A.S. (2006). Elevated levels of two tRNA species bypass the requirement for elongator complex in transcription and exocytosis. Mol. Cell *24*, 139–148.

Fox, J.W., Lamperti, E.D., Eksioglu, Y.Z., Hong, S.E., Feng, Y., Graham, D.A., Scheffer, I.E., Dobyns, W.B., Hirsch, B.A., Radtke, R.A., et al. (1998). Mutations in filamin 1 prevent migration of cerebral cortical neurons in human periventricular heterotopia. Neuron *21*, 1315–1325.

Fujita, T., Maturana, A.D., Ikuta, J., Hamada, J., Walchli, S., Suzuki, T., Sawa, H., Wooten, M.W., Okajima, T., Tatematsu, K., et al. (2007). Axonal guidance protein FEZ1 associates with tubulin and kinesin motor protein to transport mitochondria in neurites of NGF-stimulated PC12 cells. Biochem. Biophys. Res. Commun. *361*, 605–610.

Gaertig, J., Cruz, M.A., Bowen, J., Gu, L., Pennock, D.G., and Gorovsky, M.A. (1995). Acetylation of lysine 40 in alpha-tubulin is not essential in Tetrahymena thermophila. J. Cell Biol. *129*, 1301–1310.

Gardiner, J., Barton, D., Marc, J., and Overall, R. (2007). Potential role of tubulin acetylation and microtubule-based protein trafficking in familial dysautonomia. Traffic *8*, 1145–1149.

Gleeson, J.G., Allen, K.M., Fox, J.W., Lamperti, E.D., Berkovic, S., Scheffer, I., Cooper, E.C., Dobyns, W.B., Minnerath, S.R., Ross, M.E., et al. (1998). Doublecortin, a brain-specific gene mutated in human X-linked lissencephaly and double cortex syndrome, encodes a putative signaling protein. Cell *92*, 63–72.

Gomes, R.A., Hampton, C., El-Sabeawy, F., Sabo, S.L., and McAllister, A.K. (2006). The dynamic distribution of TrkB receptors before, during, and after synapse formation between cortical neurons. J. Neurosci. *26*, 11487–11500.

Haggarty, S.J., Koeller, K.M., Wong, J.C., Grozinger, C.M., and Schreiber, S.L. (2003). Domain-selective small-molecule inhibitor of histone deacetylase 6 (HDAC6)-mediated tubulin deacetylation. Proc. Natl. Acad. Sci. USA *100*, 4389–4394.

Hawkes, N.A., Otero, G., Winkler, G.S., Marshall, N., Dahmus, M.E., Krappmann, D., Scheidereit, C., Thomas, C.L., Schiavo, G., Erdjument-Bromage, H., et al. (2002). Purification and characterization of the human elongator complex. J. Biol. Chem. *277*, 3047–3052.

Hayashi, K., Ohshima, T., and Mikoshiba, K. (2002). Pak1 is involved in dendrite initiation as a downstream effector of Rac1 in cortical neurons. Mol. Cell. Neurosci. *20*, 579–594.

Huang, B., Johansson, M.J., and Bystrom, A.S. (2005). An early step in wobble uridine tRNA modification requires the Elongator complex. RNA *11*, 424–436.

Hubbert, C., Guardiola, A., Shao, R., Kawaguchi, Y., Ito, A., Nixon, A., Yoshida, M., Wang, X.F., and Yao, T.P. (2002). HDAC6 is a microtubule-associated deacetylase. Nature *417*, 455–458.

Johansen, L.D., Naumanen, T., Knudsen, A., Westerlund, N., Gromova, I., Junttila, M., Nielsen, C., Bottzauw, T., Tolkovsky, A., Westermarck, J., et al. (2008). IKAP localizes to membrane ruffles with filamin A and regulates actin cytoskeleton organization and cell migration. J. Cell Sci. *121*, 854–864.

Keays, D.A., Tian, G., Poirier, K., Huang, G.J., Siebold, C., Cleak, J., Oliver, P.L., Fray, M., Harvey, R.J., Molnar, Z., et al. (2007). Mutations in alpha-tubulin cause abnormal neuronal migration in mice and lissencephaly in humans. Cell *128*, 45–57.

Kim, J.H., Lane, W.S., and Reinberg, D. (2002). Human Elongator facilitates RNA polymerase II transcription through chromatin. Proc. Natl. Acad. Sci. USA *99*, 1241–1246.

Kim, S.C., Sprung, R., Chen, Y., Xu, Y., Ball, H., Pei, J., Cheng, T., Kho, Y., Xiao, H., Xiao, L., et al. (2006). Substrate and functional diversity of lysine acetylation revealed by a proteomics survey. Mol. Cell *23*, 607–618.

Kouskouti, A., and Talianidis, I. (2005). Histone modifications defining active genes persist after transcriptional and mitotic inactivation. EMBO J. *24*, 347–357.

Kozminski, K.G., Diener, D.R., and Rosenbaum, J.L. (1993). High level expression of nonacetylatable alpha-tubulin in Chlamydomonas reinhardtii. Cell Motil. Cytoskeleton *25*, 158–170.

Kristjuhan, A., and Svejstrup, J.Q. (2004). Evidence for distinct mechanisms facilitating transcript elongation through chromatin in vivo. EMBO J. *23*, 4243–4252.

Lom, B., and Cohen-Cory, S. (1999). Brain-derived neurotrophic factor differentially regulates retinal ganglion cell dendritic and axonal arborization in vivo. J. Neurosci. *19*, 9928–9938.

LoTurco, J.J., and Bai, J. (2006). The multipolar stage and disruptions in neuronal migration. Trends Neurosci. *29*, 407–413.

Marin, O., and Rubenstein, J.L. (2003). Cell migration in the forebrain. Annu. Rev. Neurosci. *26*, 441–483.

Mezey, E., Parmalee, A., Szalayova, I., Gill, S.P., Cuajungco, M.P., Leyne, M., Slaugenhaupt, S.A., and Brownstein, M.J. (2003). Of splice and men: what does the distribution of IKAP mRNA in the rat tell us about the pathogenesis of familial dysautonomia? Brain Res. *983*, 209–214.

Nagano, T., Morikubo, S., and Sato, M. (2004). Filamin A and FILIP (Filamin A-Interacting Protein) regulate cell polarity and motility in neocortical subventricular and intermediate zones during radial migration. J. Neurosci. *24*, 9648–9657.

Nguyen, L., Besson, A., Heng, J.I., Schuurmans, C., Teboul, L., Parras, C., Philpott, A., Roberts, J.M., and Guillemot, F. (2006). p27kip1 independently promotes neuronal differentiation and migration in the cerebral cortex. Genes Dev. *20*, 1511–1524.

North, B.J., Marshall, B.L., Borra, M.T., Denu, J.M., and Verdin, E. (2003). The human Sir2 ortholog, SIRT2, is an NAD+-dependent tubulin deacetylase. Mol. Cell *11*, 437–444.

North, B.J., and Verdin, E. (2007). Mitotic regulation of SIRT2 by cyclin-dependent kinase 1-dependent phosphorylation. J. Biol. Chem. *282*, 19546–19555.

Petrakis, T.G., Wittschieben, B.O., and Svejstrup, J.Q. (2004). Molecular architecture, structure-function relationship, and importance of the Elp3 subunit for the RNA binding of holo-elongator. J. Biol. Chem. *279*, 32087–32092.

Rahl, P.B., Chen, C.Z., and Collins, R.N. (2005). Elp1p, the yeast homolog of the FD disease syndrome protein, negatively regulates exocytosis independently of transcriptional elongation. Mol. Cell *17*, 841–853.

Reed, N.A., Cai, D., Blasius, T.L., Jih, G.T., Meyhofer, E., Gaertig, J., and Verhey, K.J. (2006). Microtubule acetylation promotes kinesin-1 binding and transport. Curr. Biol. *16*, 2166–2172.

Reiner, O., Carrozzo, R., Shen, Y., Wehnert, M., Faustinella, F., Dobyns, W.B., Caskey, C.T., and Ledbetter, D.H. (1993). Isolation of a Miller-Dieker lissencephaly gene containing G protein beta-subunit-like repeats. Nature *364*, 717–721.

Roy, S., Coffee, P., Smith, G., Liem, R.K., Brady, S.T., and Black, M.M. (2000). Neurofilaments are transported rapidly but intermittently in axons: implications for slow axonal transport. J. Neurosci. *20*, 6849–6861.

Shu, T., Tseng, H.C., Sapir, T., Stern, P., Zhou, Y., Sanada, K., Fischer, A., Coquelle, F.M., Reiner, O., and Tsai, L.H. (2006). Doublecortin-like kinase controls neurogenesis by regulating mitotic spindles and M phase progression. Neuron *49*, 25–39.

Slaugenhaupt, S.A., Blumenfeld, A., Gill, S.P., Leyne, M., Mull, J., Cuajungco, M.P., Liebert, C.B., Chadwick, B., Idelson, M., Reznik, L., et al. (2001). Tissue-specific expression of a splicing mutation in the IKBKAP gene causes familial dysautonomia. Am. J. Hum. Genet. *68*, 598–605.

Slaugenhaupt, S.A., and Gusella, J.F. (2002). Familial dysautonomia. Curr. Opin. Genet. Dev. *12*, 307–311.

Svejstrup, J.Q. (2007). Elongator complex: how many roles does it play? Curr. Opin. Cell Biol. *19*, 331–336.

Tabata, H., and Nakajima, K. (2003). Multipolar migration: the third mode of radial neuronal migration in the developing cerebral cortex. J. Neurosci. *23*, 9996–10001.

Vaquero, A., Scher, M.B., Lee, D.H., Sutton, A., Cheng, H.L., Alt, F.W., Serrano, L., Sternglanz, R., and Reinberg, D. (2006). SirT2 is a histone deacetylase with preference for histone H4 Lys 16 during mitosis. Genes Dev. *20*, 1256–1261.

Winkler, G.S., Kristjuhan, A., Erdjument-Bromage, H., Tempst, P., and Svejstrup, J.Q. (2002). Elongator is a histone H3 and H4 acetyltransferase important for normal histone acetylation levels in vivo. Proc. Natl. Acad. Sci. USA *99*, 3517–3522.

Wittschieben, B.O., Otero, G., de Bizemont, T., Fellows, J., Erdjument-Bromage, H., Ohba, R., Li, Y., Allis, C.D., Tempst, P., and Svejstrup, J.Q. (1999). A novel histone acetyltransferase is an integral subunit of elongating RNA polymerase II holoenzyme. Mol. Cell *4*, 123–128.

Wittschieben, B.O., Fellows, J., Du, W., Stillman, D.J., and Svejstrup, J.Q. (2000). Overlapping roles for the histone acetyltransferase activities of SAGA and elongator in vivo. EMBO J. *19*, 3060–3068.

Yokota, Y., Ring, C., Cheung, R., Pevny, L., and Anton, E.S. (2007). Nap1-regulated neuronal cytoskeletal dynamics is essential for the final differentiation of neurons in cerebral cortex. Neuron *54*, 429–445.

Zhang, Y., Li, N., Caron, C., Matthias, G., Hess, D., Khochbin, S., and Matthias, P. (2003). HDAC-6 interacts with and deacetylates tubulin and microtubules in vivo. EMBO J. *22*, 1168–1179.